Adaptive hybrid synchronisation in uncertain Kuramoto networks with limited information

Baldi, Simone; Tao, Tian; Kosmatopoulos, Elias B.

DOI
10.1049/iet-cta.2018.5465

Publication date
2019

Document Version
Accepted author manuscript

Published in
IET Control Theory and Applications

IET Research Journals

Submission Template for IET Research Journal Papers

IET Journals
The Institution of Engineering and Technology

ISSN 1751-8644
doi: 0000000000
www.ietdl.org

Adaptive hybrid synchronization in uncertain Kuramoto networks with limited information

Simone Baldi[1*], *Tian Tao*[1], *Elias B. Kosmatopoulos*[2]

[1] *Delft Center for Systems and Control, Delft University of Technology, Delft, 2628CD, The Netherlands*
[2] *Department of Electrical and Computer Engineering, Democritus University of Thrace, Xanthi, 67100 Greece, and Informatics & Telematics Institute, Center for Research and Technology Hellas (ITI-CERTH), Thessaloniki 57001, Greece*
* *E-mail: s.baldi@tudelft.nl*

Abstract: In this work we study adaptive synchronization in networks with Kuramoto units whose parameters are unknown and where measurements are quantized over the communication network (therefore information is limited). We show that, for an undirected connected graph, synchronization is enabled via appropriate adaptive protocols that counteract the effect of heterogeneity, uncertainty, and quantized information. In particular, to address heterogeneity and uncertainty, appropriate adaptive laws are designed to drive the network to frequency synchronization; to address quantized information, a dynamic quantizer is introduced and embedded into the adaptive mechanism via a zooming-based approach (therefore with hybrid dynamics). The resulting protocol ends up being an adaptive hybrid synchronization strategy that can be distributed throughout the network: the quantizer is co-designed with the controller, as typical for zooming-based quantization. The proposed integrated adaptation+quantization protocol guarantees asymptotic synchronization to a desired frequency, which is shown via an appropriately designed distributed Lyapunov function. Numerical simulations are also used to demonstrate the effectiveness of the proposed protocol.
Keywords: Adaptive synchronization, Kuramoto dynamics, uncertain systems, quantization, adaptive hybrid control.

1 Introduction

Synchronization is a collective phenomenon occurring in systems of interacting units [1–4]. Synchronization can be leaderless [5] or leader-follower [6, 7]: in the second case the network is steered in some desired and a priori known solution defined by a leader unit. In the 80's Kuramoto proposed an exactly solvable model of collective synchronization, which became known as the Kuramoto model [8]: this model has been adopted in many fields like swarms [9], smart grids [10, 11], among others [12].

Most synchronization models for non-evolving (or non-adaptive) Kuramoto or Kuramoto-like networks (e.g. networks of phase oscillators) have shown that synchronization is favored if the coupling strength among the units is large enough and the spectrum of variety of the oscillators is narrow: this last point amounts to assuming homogeneous or almost homogeneous oscillators [13]. However, real-world networks have uncertain and heterogeneous parameters which might even change with time. Therefore, in place of static couplings, researchers have later been focusing on Kuramoto or Kuramoto-like networks characterized by evolving, adapting couplings which vary in time according to different environmental conditions, leading to the study of evolving (or adaptive) networks [14–16]. In [17] a simple model of adaptive Kuramoto network is given via mechanisms of homophily (reinforcing interactions with correlated units) and homeostasis (preserving the overall connection strength). In [18] a set of adaptive strategies for synchronization and consensus of complex networks of dynamical systems is presented. The authors in [19] devise an adaptive scheme to achieve phase synchronization by suppressing the negative effect of the heterogeneity in the network, while in [20] protocols are designed to adaptively interact with system dynamics and preserve the sum of all incoming pairwise coupling strengths. In [21] a co-evolutionary rewiring strategy that depends only on the phase differences of neighboring oscillators is studied for Kuramoto units. However, adaptive synchronization of heterogeneous Kuramoto networks is usually shown numerically but not analytically proven.

Within the scope of synchronization, this work will be focusing on how to achieve adaptive synchronization in uncertain and heterogeneous Kuramoto networks in the presence of networked-induced quantization. Established approaches to quantization rely on dynamic quantization mechanisms such as logarithmic quantization [22], or zooming-based hybrid control [23]. The latter mechanism takes its name from the analogy with the zooming in digital cameras: when the state is outside its range region, the quantizer 'zooms out' so that the state can be captured within the region. On the other hand, once the state comes close to the origin, we can 'zoom in' by reducing the size of the range so that the quantization resolution becomes finer while the region becomes smaller. Repeating this zooming in, we can obtain asymptotic stabilization. Recently, adaptive approaches to quantization have been proposed for standalone systems via different techniques, namely passification-based adaptive control [24, 25], direct adaptive control [26–28], adaptive backstepping [29, 30], or sliding mode [31]. However, such approaches have not been studied for networks of uncertain and heterogeneous units. In fact, for network systems, while several approaches to synchronization with quantized measurements can be found in literature [32–34], to the best of the authors' knowledge, none of them is dealing with parametric uncertainty, which motivates this work.

In this work we study adaptive synchronization in undirected connected networks with Kuramoto units whose parameters are unknown and where information is quantized over the communication network. Synchronization is enabled via appropriate adaptive hybrid protocols in the presence of both heterogeneous and uncertain dynamics. To address quantized information a dynamic quantizer is introduced and embedded into the adaptive mechanism via a zooming-based approach. the quantizer is co-designed with the controller, i.e. the quantizer parameters are part of the design process. This is the typical approach used both in logarithmic and zooming-based quantization [22, 23]. The main contributions of this work are the following: (a) proving asymptotic synchronization of Kuramoto units in an adaptive way and with quantized information; (b) adopting a Lyapunov function that allows to distribute the dynamic

quantization strategy using only local information. The main benefit of the proposed integrated adaptation+quantization protocol is to guarantee asymptotic synchronization, whereas in the absence of any dynamic quantization mechanism, one would obtain at most bounded synchronization error.

The rest of the paper is organized as follows. Sect. 2 provides the problem formulation. Synchronization protocols are given in Sects. 3 and 4 without and with quantization, respectively. Numerical examples are in Sect. 5, and Sect. 6 concludes the work.

Notation: The notation in this paper is standard. The transpose of a matrix or of a vector is indicated with X^T and x^T respectively. A vector signal $x \in \mathbb{R}^n$ is said to belong to $\mathscr{L}_\infty$ class ($x \in \mathscr{L}_\infty$), if $\max_{t\geq 0} \|x(t)\| < \infty$, $\forall t \geq 0$. A time-invariant undirected communication graph of order N is completely defined by the pair $\mathscr{G} = (\mathscr{V}, \mathscr{E})$, where $\mathscr{V} = \{1, \ldots, N\}$ is a finite nonempty set of nodes, and $\mathscr{E} \subseteq \mathscr{V} \times \mathscr{V}$ is a set of corresponding non-ordered pair of nodes, called edges. The adjacency matrix of a weighted undirected graph $\mathscr{K} = [k_{ij}]$ is defined as $k_{ii} = 0$ and $k_{ij} = k_{ji} > 0$ if $(i, j) \in \mathscr{E}$, where $i \neq j$. The adjacency matrix $\mathscr{A} = [a_{ij}]$ of an unweighted undirected graph is defined as $a_{ii} = 0$ and $a_{ij} = a_{ji} = 1$ if $(i, j) \in \mathscr{E}$, where $i \neq j$. The Laplacian matrix of the unweighted graph is defined as $\mathscr{L} = [l_{ij}]$, where $l_{ii} = \sum_j a_{ij}$ and $l_{ij} = -a_{ij}$, if $i \neq j$. An undirected graph $\mathscr{G}$ is said to be connected if, taken any arbitrary pair of nodes (i, j) where $i, j \in \mathscr{V}$, there is a path that leads from i to j.

2 Problem formulation

The following network of heterogeneous coupled oscillators with unknown dynamics is considered in this work

$$\begin{aligned} & m_i\ddot{\theta}_i + d_i\dot{\theta}_i = \tau_i - \sum_{j=1}^{N} k_{ij}\sin(\theta_i - \theta_j), \\ & i \in \mathscr{V} \triangleq \{1, 2, \ldots, N\} \end{aligned} \tag{1}$$

where the time index t may be omitted whenever obvious. The meaning of the parameters in (1) can be examined via the mechanical analogy of mass points in Figure 1. After neglecting any collision,

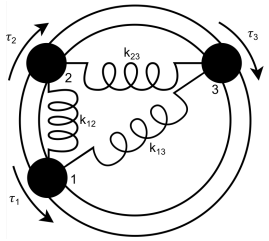

Fig. 1: Mechanical analogy of a network of three coupled oscillators.

each point, or unit, will move on the circle describing an angle (or phase, by analogy) θ_i and an angular velocity (or frequency, by analogy) $\dot{\theta}_i$, under the effect of an external driving torque τ_i, an elastic restoring torque $k_{ij}\sin(\theta_i - \theta_j)$ (with $k_{ij} = k_{ji}$), and a viscous damping torque $d_i\dot{\theta}_i$ that is opposite to the direction of motion. All inertial coefficients m_i, damping coefficients d_i and stiffness coefficients k_{ij} have positive but *unknown* value. The external driving torque has two components

$$\tau_i = \omega_i + u_i, \qquad i \in \mathscr{V} \tag{2}$$

where u_i is the actual control torque and ω_i is a term proportional to the natural angular velocity (or natural frequency) of the unit i, that is the angular velocity it would have if there were no couplings. Let us define for convenience the state $x_i = \dot{\theta}_i$. Then, (1) can be rewritten as

$$\dot{x}_i = -\frac{d_i}{m_i}x_i + \frac{1}{m_i}\left(u_i + \omega_i - \sum_{j=1}^{N} k_{ij}\sin(\theta_i - \theta_j)\right) \tag{3}$$

The following connectivity assumption is made.

Assumption 1. The graph $\mathscr{G}$ of the network of Kuramoto oscillators (1) is undirected and connected. In addition, let us assume that the network through which the oscillators can exchange information coincides with the network through which the oscillators are physically coupled.

The following assumption on the uncertainty set is made.

Assumption 2. Upper bounds for the positive constants m_i, d_i and k_{ij}, call them $\bar{m}_i$, $\bar{d}_i$ and $\bar{k}_{ij}$ are known. Let us call the resulting uncertainty set Θ_i for compactness.

Remark 1. *Assumption 1 is a standard connectivity assumption required for convergence of consensus dynamics. Assumption 2 is required to obtain a bound to the increasing rate of the tracking error during the zooming in phase, as it will be explained in Section 4.*

Quantized information is now introduced. Let $z \in \mathbb{R}^n$ be the variable being quantized. The uniform static quantizer is described by a function $g : \mathbb{R}^n \to Q$, where $Q \subset \mathbb{R}^n$. The finite set of values is defined as $\{z \in \mathbb{R}^n : q(z) = i\}$, $i \in Q$. With these considerations in mind, we define the following dynamic quantizer:

$$q_\mu(z) = \mu q\left(\frac{z}{\mu}\right) \tag{4}$$

where $\mu > 0$. Note that the dynamic quantizer (4) satisfies the following condition:

$$\mu\left\|q\left(\frac{z}{\mu}\right)\right\| \leq \mu M \tag{5}$$

where μM represents the quantization range and $M > 0$ is the quantization range of the static quantizer $g(z)$. The quantization range M and quantization error Δ will be adjusted by using a hybrid control policy defined in Section 4.

We are now ready to formulate the synchronization problem.

Problem 1. [*Adaptive frequency synchronization*] Consider a network of unknown oscillators (1) satisfying Assumptions 1 and 2. Find a distributed adaptive strategy (i.e. exploiting only measurements from neighbors) for the control input u_i such that the network frequency synchronizes to an a priori defined frequency x_0, i.e. $x_i - x_0 \to 0$, $\forall i$. In addition, assuming that information is quantized over the communication network according to (4), find a distributed adaptive strategy for the control input u_i and for the dynamic parameter μ_i such that $x_i - x_0 \to 0$, $\forall i$.

A result is now given which is instrumental to solving the problem above.

Proposition 1. [*Homogeneization*] There exists a family of scalars $k_i^* \in \mathbb{R}$ and $l_i^* > 0$ such that

$$\begin{cases} -\dfrac{d_i}{m_i} + \dfrac{1}{m_i}k_i^* = 0 \\ \qquad\quad l_i^*\dfrac{1}{m_i} = 1 \end{cases} \tag{6}$$

Furthermore, there exists an ideal controller

$$u_i^* = k_i^*\dot{\theta}_i - l_i^*\sum_{j=1}^{N} a_{ij}(\dot{\theta}_i - \dot{\theta}_j) + c_i^* + \sum_{j=1}^{N} g_{ij}^* a_{ij}\sin(\theta_i - \theta_j) \tag{7}$$

with $c_i^* = -\omega_i$, $g_{ij}^* = k_{ij}$ which leads to the following dynamics

$$\dot{x}_i = -\sum_{j=1}^{N} a_{ij}(x_i - x_j) \tag{8}$$

Proof: The proof directly follows from applying the control input (7) to unit (3), and using (6).

Remark 2. *Conditions* (6) *basically correspond to matching the uncertain dynamics to first-order consensus dynamics* (8) *for which leaderless synchronization ($x_i - x_j \to 0$, $\forall i, j$) has been well studied in literature [35]. It is not difficult to show that the controller*

$$\begin{aligned} u_i^* = k_i^* \dot{\theta}_i - l_i^* \sum_{j=1}^{N} a_{ij}(\dot{\theta}_i - \dot{\theta}_j) - l_i^*(\dot{\theta}_i - \dot{\theta}_0) \\ + c_i^* + \sum_{j=1}^{N} g_{ij}^* a_{ij} \sin(\theta_i - \theta_j) \end{aligned} \tag{9}$$

where $\dot{\theta}_0$ is constant and a priori given, leads to leader-follower synchronization dynamics

$$\dot{x}_i = -\sum_{j=0}^{N} a_{ij}(x_i - x_j) \tag{10}$$

where $a_{i0} = 1$ $\forall i$ by definition, which guarantees convergence of all $\dot{\theta}_i$ to $\dot{\theta}_0$ [35]. The connectivity assumption (Assumption 1) is instrumental in guaranteeing convergence of the dynamics (10)*, which turn out to be leader-follower consensus dynamics [36, 37].*

Remark 3. *It is worth mentioning that, since m_i, d_i, ω_i, k_{ij} are unknown, the ideal control* (7) *cannot be implemented to solve Problem 1. Therefore, some adaptation mechanisms must be devised to estimate the unknown ideal gains in Proposition 1 by exploiting only measurements from neighbors. This is shown in the next section.*

3 Distributed adaptive synchronization

The following synchronizing protocol is proposed

$$\begin{aligned} u_i(t) = & k_i(t)\dot{\theta}_i - l_i(t) \sum_{j=1}^{N} a_{ij}(\dot{\theta}_i(t) - \dot{\theta}_j(t)) - l_i(t)(\dot{\theta}_i - \dot{\theta}_0) \\ & + c_i(t) + \sum_{j=1}^{N} g_{ij}(t) a_{ij} \sin(\theta_i(t) - \theta_j(t)) \end{aligned} \tag{11}$$

where k_i, l_i, c_i, g_{ij}, are the (time-dependent) estimates of k_i^*, l_i^*, c_i^*, g_{ij}^*, respectively. The following synchronization result holds.

Theorem 1. *Define the errors*

$$e_i = \sum_{j=0}^{N} a_{ij}(\dot{\theta}_i - \dot{\theta}_j), \qquad e = [e_1, e_2, \ldots, e_N]^T. \tag{12}$$

Under Assumption 1, the heterogeneous Kuramoto network (3)*, controlled using the synchronizing protocol* (11) *and the following adaptive laws*

$$\begin{aligned} \dot{k}_i &= \mathscr{P}_{\Theta_i}\left[-\gamma\left(\sum_{j=0}^{N} a_{ij}(e_i - e_j)\right)\dot{\theta}_i\right] \\ \dot{l}_i &= \mathscr{P}_{\Theta_i}\left[\gamma\left(\sum_{j=0}^{N} a_{ij}(e_i - e_j)\right) e_i\right] \\ \dot{c}_i &= \mathscr{P}_{\Theta_i}\left[-\gamma\left(\sum_{j=0}^{N} a_{ij}(e_i - e_j)\right)\right] \\ \dot{g}_{ij} &= \mathscr{P}_{\Theta_i}\left[-\gamma\left(\sum_{j=0}^{N} a_{ij}(e_i - e_j)\right)\sin(\theta_i - \theta_j)\right] \end{aligned} \tag{13}$$

where $\mathscr{P}_{\Theta_i}$ represent parameter projection in the uncertainty set Θ_i, and $\gamma > 0$ is the adaptive gain, reaches frequency synchronization ($\dot{\theta}_i - \dot{\theta}_0 \to 0$, $\forall i$).

Proof: The closed-loop network formed by (3) and (11) is

$$\begin{aligned} \dot{x}_i = & \left(-\frac{d_i}{m_i} + \frac{1}{m_i}k_i\right)x_i - l_i\frac{1}{m_i}\sum_{j=1}^{N} a_{ij}(x_i - x_j) - l_i\frac{1}{m_i}(x_i - x_0) \\ & + \frac{1}{m_i}(c_i + \omega_i) + \frac{1}{m_i}\sum_{j=1}^{N} a_{ij}(g_{ij} - k_{ij})\sin(\theta_i - \theta_j) \end{aligned} \tag{14}$$

which can be rewritten as a function of the estimation errors,

$$\begin{aligned} \dot{x}_i = & \frac{1}{m_i}\tilde{k}_i(t)x_i - (\tilde{l}_i(t)\frac{1}{m_i} - 1)\sum_{j=1}^{N} a_{ij}(x_i - x_j) + \frac{1}{m_i}\tilde{c}_i(t) - \\ & (\tilde{l}_i(t)\frac{1}{m_i} - 1)(x_i - x_0) + \frac{1}{m_i}\sum_{j=1}^{N} \tilde{g}_{ij}(t) a_{ij}\sin(\theta_i - \theta_j) \end{aligned} \tag{15}$$

where $\tilde{k}_i(t) = k_i(t) - k_i^*$, $\tilde{l}_i(t) = l_i(t) - l_i^*$, $\tilde{c}_i(t) = c_i(t) - c_i^*$, $\tilde{g}_{ij}(t) = g_{ij}(t) - g_{ij}^*$. By defining for compactness

$$\begin{aligned} B_k(t) &= \mathrm{diag}(\frac{1}{m_1}\tilde{k}_1(t), \ldots, \frac{1}{m_N}\tilde{k}_N(t)) \\ B_l(t) &= \mathrm{diag}(-\tilde{l}_1(t)\frac{1}{m_1}, \ldots, -\tilde{l}_N(t)\frac{1}{m_N}) \\ B_c(t) &= \mathrm{diag}(\frac{1}{m_1}\tilde{c}_1(t), \ldots, \frac{1}{m_N}\tilde{c}_N(t)) \\ B_g(t) &= \mathrm{diag}(\frac{1}{m_1}\sum_{j=1}^{N}\tilde{g}_{1j}(t)a_{1j}\sin(\theta_1 - \theta_j), \ldots \\ & \ldots, \frac{1}{m_N}\sum_{j=1}^{N}\tilde{g}_{Nj}(t)a_{Nj}\sin(\theta_N - \theta_j)) \end{aligned} \tag{16}$$

the closed-loop for the overall network can be written as

$$\dot{x} = B_k(t)x + (-I_N + B_l(t))e + B_c(t) + B_g(t) \tag{17}$$

where $x = [x_1, x_2, \ldots, x_N]^T$. Recalling that the synchronization error is $e = I_N(x - \bar{x}_0) + \mathscr{L}x$, where $\bar{x}_0 = [x_0, x_0, \ldots, x_0]^T$, the error

dynamics are

$$\begin{aligned}\dot{e} = &-(I_N+\mathscr{L})e+\\ &+(I_N+\mathscr{L})(B_k(t)x+B_l(t)e+B_c(t)+B_g(t)).\end{aligned} \tag{18}$$

The adaptive laws (13) arise from considering the Lyapunov function candidate

$$\begin{aligned}V = &\sum_{i=1}^{N} e_i^2(t)+\sum_{i=1}^{N}\frac{\tilde{k}_i^2(t)\gamma^{-1}}{|l_i^*|}+\sum_{i=1}^{N}\frac{\tilde{l}_i^2(t)\gamma^{-1}}{|l_i^*|}\\ &+\sum_{i=1}^{N}\frac{\tilde{c}_i^2(t)\gamma^{-1}}{|l_i^*|}+\sum_{i=1}^{N}\sum_{j=1}^{N}\frac{\tilde{g}_{ij}^2(t)\gamma^{-1}}{|l_i^*|}.\end{aligned} \tag{19}$$

Then we have

$$\begin{aligned}2e^T\dot{e} = &-2e^T(I_N+\mathscr{L})e+\\ &+2e^T(I_N+\mathscr{L})(B_kx+B_le+B_c+B_g)\end{aligned} \tag{20}$$

and

$$\begin{aligned}\dot{V} \leq &-2\sum_{i=1}^{N}\underline{\sigma}(I_N+\mathscr{L})e_i^2\\ &+2\sum_{i=1}^{N}\frac{\tilde{k}_i(t)}{|l_i^*|}\left[\gamma^{-1}\dot{\tilde{k}}_i(t)+x_i\left(\sum_{j=0}^{N}a_{ij}(e_i-e_j)\right)\right]\\ &+2\sum_{i=1}^{N}\frac{\tilde{l}_i(t)}{|l_i^*|}\left[\gamma^{-1}\dot{\tilde{l}}_i(t)-e_i\left(\sum_{j=0}^{N}a_{ij}(e_i-e_j)\right)\right]\\ &+2\sum_{i=1}^{N}\frac{\tilde{c}_i(t)}{|l_i^*|}\left[\gamma^{-1}\dot{\tilde{c}}_i(t)+\left(\sum_{j=0}^{N}a_{ij}(e_i-e_j)\right)\right]+2\sum_{i=1}^{N}\sum_{j=1}^{N}\\ &\frac{\tilde{g}_{ij}(t)}{|l_i^*|}\left[\gamma^{-1}\dot{\tilde{g}}_{ij}(t)+\sin(\theta_i-\theta_j)\left(\sum_{j=0}^{N}a_{ij}(e_i-e_j)\right)\right]\end{aligned} \tag{21}$$

where $\underline{\sigma}(\cdot)$ is a real number representing the smallest eigenvalue of a square symmetric matrix. Using (13) we have

$$\dot{V} \leq -2\sum_{i=1}^{N}\underline{\sigma}(I_N+\mathscr{L})e_i^2 \tag{22}$$

which is negative semi-definite. Using standard Lyapunov arguments we can prove boundedness of all closed-loop signals and convergence of e to 0. In fact, since $V>0$ and $\dot{V}\leq 0$, it follows that $V(t)$ has a limit, i.e. $\lim_{t\to\infty}V(e(t),\tilde{\Omega}(t))=V_\infty<\infty$, where we have collected all parametric errors in $\tilde{\Omega}$. The finite limit implies V, e, $\tilde{\Omega}\in\mathscr{L}_\infty$. In addition, since $\dot{V}$ is uniformly continuous in time (this is satisfied because $\ddot{V}$ is finite), the Barbalat's lemma implies $\dot{V}\to 0$ as $t\to\infty$ and hence $e\to 0$, from which we derive $x_i\to x_0$, $\forall i$. This concludes the proof.

Remark 4. *Theorem 1 provides a leader-follower synchronization protocol driving the synchronization error to zero. In standard leader-follower synchronization protocols, the desired reference is available to a single node (or to a few nodes) in the team acting as leader(s). However, traditionally, the literature on Kuramoto oscillators has considered the reference to be available to all nodes: see for example the relevant works [38, 39]. Here, the pacemaker provides a reference frequency to all nodes: such a setting is justified in view of the fact that Kuramoto models are often used in smart grid applications [40, 41]. In this scenario, $\dot{\theta}_0$ represents the globally-known 50 or 60 Hz to be followed by all systems. In line with such literature, also in the proposed protocol the knowledge of $\dot{\theta}_0$ is available to all systems in the network: nevertheless, using a distributed observer, it is not difficult to extend the proposed approach to the setting where the desired reference is available to a single or to a few nodes. This issue was studied by some of the authors in [16]. With a similar smart grid application in mind, we have been focusing on frequency synchronization, rather than on full-state (phase and frequency) synchronization. The proposed protocol requires the measurements of both θ_i and $\dot{\theta}_i$. This might sound demanding, but many management algorithms in smart grids (frequency regulation, optimal power flow, etc.) require both θ_i and $\dot{\theta}_i$. In addition, because of the widespread use of phasor measurement units (PMUs), it is nowadays quite straightforward to measure θ_i and $\dot{\theta}_i$ in smart grids. A PMU is a device which measures the electrical waves on an electricity grid.*

Remark 5. *Note that the parameter projection $\mathscr{P}_{\Theta_i}[\cdot]$ in* (13) *is not necessary for stability. As a matter of fact, stability can be achieved evn without any projection $\mathscr{P}_{\Theta_i}[\cdot]$ (see for example the full-state synchronization strategy in [16]). However, since parameter projection is fundamental for stability in the presence of quantized information as explained in the next section, then parameter projection has been introduced in Theorem 1 as well.*

Remark 6. *In order to implement* (13)*, and in particular the term $\sum_{j=1}^{N}a_{ij}(e_i-e_j)$, it is required to communicate among neighbors the extra variable e_i. In fact, the variable e_i can also be thought to be local information for the following rationale. Communication of extra local variables is often at the core of many synchronization protocols: for example, synchronization based on distributed observer [42, 43] requires communication of extra local variables representing the observer states. Therefore, communication of e_i is homologous to communication of any other auxiliary variable. It has to be noted that, in our setting, communication of the local variable e_i is equivalent to communicating x_i to the neighbors of the neighbors (2-hop communication). This apparently more complex communication architecture actually brings a crucial useful feature: the Lyapunov function V in* (19) *ends up being block-diagonal (no synchronization error cross terms among units are present, and similarly no parameter estimation error cross terms among units are present). This reminds of the typical block-diagonal design in consensus problems, $V=e'(I\otimes P)e$ [35, 44], and it is thus consistent with such literature: in the next section we will see that such a feature is also crucial to implement a dynamic quantization strategy that does not require the complete knowledge of $\mathscr{L}$.*

4 Distributed adaptive synchronization with quantized information

Being the systems connected through a network, information (frequency and phase) should be exchanged among neighbors, and therefore quantized. Therefore, system i will received some quantized information from its neighbors j. In line with the work by Liberzon and Ishii [22, 23] and most literature stemming from there, a dynamic quantizer will be codesigned together with the controller, i.e. the quantizer parameters will also be part of the design. We consider the following quantization setting:

- Instead of quantizing the frequency $\dot{\theta}_j$ itself, we assume that each system j quantizes the difference with respect to $\dot{\theta}_0$, i.e. $q_\mu(\dot{\theta}_j-\dot{\theta}_0)$ which, upon synchronization, tends to zero;
- Instead of quantizing the phase θ_j itself, we assume that each system j sends a correction factor with respect to the phase increment, according to the relation

$$\theta_j(t) = b_j(t)+(\dot{\theta}_0+a_j(t))t \tag{23}$$

where $q_\mu(b_j(t))$ and $q_\mu(a_j(t))$ are the packages to be sent (y-intercept and incremental slope correction of the line) which, upon synchronization, tend to a constant and to zero, respectively.

Within this synchronization setting it is possible to reconstruct with arbitrary precision all signals, provided that the quantization range of (4) can be made arbitrarily small. When information is quantized according to (4), the closed-loop system (14) modifies into

$$\begin{aligned}\dot{x}_i =&(-\frac{d_i}{m_i}+\frac{1}{m_i}k_i)x_i - l_i\frac{1}{m_i}\sum_{j=1}^{N}a_{ij}(x_i-x_j) - l_i\frac{1}{m_i}(x_i-x_0)\\ &+\frac{1}{m_i}(c_i+\omega_i)+\frac{1}{m_i}\sum_{j=1}^{N}a_{ij}(g_{ij}-k_{ij})\sin(\theta_i-\theta_j)-\mu_i l_i\frac{1}{m_i}\Delta_{z_i}\end{aligned} \tag{24}$$

where Δ_z is defined as the quantization error, and in case of no saturation* it holds $\|\Delta_{z_i}\| \leq \Delta$. Note that μ_i represents the quantization range for system i.

In view of (24), the evolution of the synchronization error can be written as:

$$\begin{aligned}\dot{e} =&-(I_N+\mathscr{L})e+\\ &+(I_N+\mathscr{L})(B_k(t)x+B_l(t)e+B_c(t)+B_g(t)+B_{l\mu}(t))\end{aligned} \tag{25}$$

where we have used the same variables defined in (26), and in addition

$$B_{l\mu}(t)=\mathrm{diag}((-1-\mu_1\tilde{l}_1(t))\frac{1}{m_1}\Delta_{z_1},\ldots,(-1-\mu_N\tilde{l}_N(t))\frac{1}{m_N}\Delta_{z_N}) \tag{26}$$

In order to analyze the stability of the closed-loop system (25), it is natural to consider the same Lyapunov function defined in (19). In addition, let us consider the same adaptation laws as in (13). After repeating similar steps as in the proof of Theorem 1, we arrive at the expression

$$\dot{V} \leq -2\sum_{i=1}^{N}\underline{\sigma}(I_N+\mathscr{L})e_i(e_i+(1+\mu_i\tilde{l}_i)\frac{1}{m_i}\Delta_{z_i}). \tag{27}$$

Because all control gains are bounded due to the projection strategy in (13), we can define $\rho_i \in \mathbb{R} \geq 0$ such that:

$$\rho_i = \max_{t\geq 0}\left\{\gamma^{-1}\frac{\tilde{k}_i^2(t)+\tilde{l}_i^2(t)+\tilde{c}_i^2(t)+\sum_{j=1}^{N}\tilde{g}_{ij}^2(t)}{|l_i^*|}\right\} \tag{28}$$

and

$$\rho = \sum_{i=1}^{N}\rho_i. \tag{29}$$

In addition, because of (19) we have

$$e^Te \leq V \leq e^Te+\rho. \tag{30}$$

The most interesting observation is that, because of the separable structure of $V=\sum_{i=1}^{N}V_i$ (V_i represent the terms in (30) related only to system i), it is possible to find 'decentralized' versions of the inequality (30), i.e.

$$e_i^2 \leq V_i \leq e_i^2+\rho_i, \quad \forall i \in \mathscr{V}. \tag{31}$$

The time derivative of V in (27) in case of no saturation can be expressed as

$$\begin{aligned}\dot{V} \leq& -2\sum_{i=1}^{N}\underline{\sigma}(I_N+\mathscr{L})e_i(e_i+(1+\tilde{l}_i)\frac{1}{m_i}\mu_i\Delta)\\ \leq& -2\sum_{i=1}^{N}|e_i|\,\underline{\sigma}(I_N+\mathscr{L})\Bigg(|e_i|-\underbrace{\frac{\overline{\sigma}(I_N+\mathscr{L})}{\underline{\sigma}(I_N+\mathscr{L})}\max_{m_i\in\Theta,i\in\mathscr{V}}\left\|1+\frac{\tilde{l}_i}{m_i}\right\|}_{R}\mu_i\Delta\Bigg)\end{aligned}$$

$$\implies \dot{V} \leq -2\sum_{i=1}^{N}|e_i|\,\underline{\sigma}(I_N+\mathscr{L})(|e_i|-\mu_i R\Delta) \tag{32}$$

where R is bounded, in view of Assumption 2. The last inequality basically reveals that the time derivative of V can also be separated into N inequalities, i.e. $\dot{V}=\sum_{i=1}^{N}\dot{V}_i$ ($\dot{V}_i$ represent the terms in (32) related only to system i). According to (5), the condition for no saturation is satisfied if the following holds:

$$|e_i| \leq \mu_i M. \tag{33}$$

We define, for each system i, the following regions:

$$\begin{aligned}\mathscr{B}_{1i}(\mu_i) &:= \left\{e_i : |e_i| \leq \mu_i M\right\}\\ \mathscr{I}_{1i}(\mu_i) &:= \left\{e_i : e_i^2 \leq \mu_i^2 M^2\right\}\\ \mathscr{B}_{2i}(\mu_i) &:= \left\{e_i : |e_i| \leq \mu_i R\Delta\right\}\\ \mathscr{I}_{2i}(\mu_i) &= \left\{e_i : e_i^2 \leq \mu_i^2 R^2\Delta^2\right\}.\end{aligned} \tag{34}$$

Note that, when

$$M > R\Delta$$

then $\mathscr{B}_2(\mu_i) \subset \mathscr{I}_2(\mu_i) \subset \mathscr{I}_1(\mu_i) \subset \mathscr{B}_1(\mu_i)$.

4.1 Main Result

Using the previously explained design, we can obtain an integrated mechanism where appropriate adaptive laws interact with a zooming-based quantizer. The following stability result can be derived.

Theorem 2. *Under Assumptions 1 and 2, consider the heterogeneous Kuramoto network* (3)*, controlled using the synchronizing protocol**

$$\begin{aligned}u_i(t) =&k_i(t)\dot{\theta}_i - l_i(t)\sum_{j=0}^{N}a_{ij}(\dot{\theta}_i(t)-q_\mu(\dot{\theta}_j(t)))\\ &+c_i(t)+\sum_{j=1}^{N}g_{ij}(t)a_{ij}\sin(\theta_i(t)-q_\mu(\theta_j(t)))\end{aligned} \tag{35}$$

*Saturation occurs when the signal z exceeds the maximum quantized level. In case of no saturation ($\|z\| \leq \mu M$), it holds $\|q_\mu(z)-z\| = \mu\|\Delta_{z_i}\| \leq \mu\Delta$.

**In the next and the following equation we use, with some abuse of notation, the symbols $q_\mu(\theta_j)$, $q_\mu(\dot{\theta}_j)$ and $q_\mu(e_j)$ to indicate variable quantized as indicated at the beginning of the section.*

and the following adaptive laws

$$\begin{aligned}
\dot{k}_i &= \mathscr{P}_{\Theta_i}\left[-\gamma\left(\sum_{j=0}^{N} a_{ij}(q_\mu(e_i-e_j))\right)\dot{\theta}_i\right]\\
\dot{l}_i &= \mathscr{P}_{\Theta_i}\left[\gamma\left(\sum_{j=0}^{N} a_{ij}(q_\mu(e_i-e_j))\right)q_\mu(e_i)\right]\\
\dot{c}_i &= \mathscr{P}_{\Theta_i}\left[-\gamma\left(\sum_{j=0}^{N} a_{ij}(q_\mu(e_i-e_j))\right)\right]\\
\dot{g}_{ij} &= \mathscr{P}_{\Theta_i}\left[-\gamma\left(\sum_{j=0}^{N} a_{ij}(q_\mu(e_i-e_j))\right)\sin(\theta_i-q_\mu(\theta_j))\right]
\end{aligned} \tag{36}$$

where $\mathscr{P}_{\Theta_i}$ represent parameter projection in the uncertainty set Θ_i, and $\gamma>0$ is the adaptive gain. If the following holds

$$M > R\Delta \tag{37}$$

then there exists an error-based hybrid quantized feedback control policy that reaches frequency synchronization ($\dot{\theta}_i-\dot{\theta}_0\to 0$, $\forall i$).

Proof: We distinguish two phases, namely the zooming-out and zooming-in phases. In the zooming-out phase μ_i is chosen so that $e_i\in\mathscr{B}_{1i}(\mu_i)$ and thus boundedness can be guaranteed. During zooming-in phase the objective is to shrink the smaller region $\mathscr{I}_{2i}(\mu_i)$ by reducing the dynamic quantizer parameter μ_i so that state-tracking properties can be concluded. The two phases are explained in the following.

Zooming-out phase: Let $\mu_i(0)=1$. If $\left|e_i(0)\right|>M$ we have saturation. In this case we make $\mu_i(t)$ increase in a piecewise fashion to dominate the growth factor of e_i, which can be seen by (24) that equals $\left|e^{\max_{m_i,d_i\in\Theta}\left|-\frac{d_i+k_i}{m_i}\right|}\right|$, where $\max_{m_i,d_i\in\Theta}\left|-\frac{d_i+k_i}{m_i}\right|$ is bounded in view of Assumption 2. There will be a time instant $t_0>0$ and a bounded $\mu_i(t_0)$ at which $e_i(t_0)\in\mathscr{I}_{1i}(\mu_i(t_0))\cap\mathscr{B}_{1i}(\mu_i(t_0))$. Because $e_i(t_0)\in\mathscr{B}_{1i}(\mu_i(t_0))$ and $\mathscr{B}_{2i}(\mu_i)\subset\mathscr{B}_{1i}(\mu_i)$ from (37), we get from (32) $\dot{V}_i\le 0$. Note that this does not imply that e_i will decrease, since V_i comprises also the parametric estimation errors. Therefore, for $t>t_0$ we might have two cases: either e_i^2 is decreasing, in which case there is no saturation and we go to zooming-in phase; or e_i^2 is increasing, in which case we keep increasing $\mu_i(t)$ at the same rate. For this second case, because $\mu_i(t)$ is updated continuously at much higher rate compared to the growth of $e_i(t)$ to avoid saturation, we can assume that $\forall t\ge t_0$, $e_i(t)\in\mathscr{B}_{1i}(\mu_i(t))$.

Zooming-in phase: Let t' be a time instant such that $t\ge t'\ge t_0$, and $e_i(t)\in\mathscr{B}_{1i}(\mu_i(t'))$. Then it is true that $\dot{V}_i\le 0$ as long as $e_i\notin\mathscr{B}_{2i}(\mu_i(t'))$. One can see from (34) that $\mathscr{B}_{2i}(\mu_i)\subset\mathscr{I}_{2i}(\mu_i)$. Thus, at time $\tilde{t}$ with $\tilde{t}\ge t'$, when $e_i(t)\in\mathscr{I}_{2i}(\mu_i(t'))$, $\mu(\tilde{t})$ is updated

$$\mu_i(\tilde{t}) = \underbrace{\frac{R\Delta}{M}}_{\Omega}\mu_i(t'). \tag{38}$$

Obviously $\Omega<1$ due to (37). Thus, zooming-in event occurs, and one can see that $\mathscr{I}_{1i}(\mu_i(\tilde{t}))=\mathscr{I}_{2i}(\mu_i(t'))$, where $\mu_i(t')$ is the value of μ_i that prevents saturation. After the zooming-in event one might have two cases: either the tracking error increases tending to violate $e_i\in\mathscr{B}_{1i}(\mu_i(\tilde{t}))$, in which case a new zooming-out phase is activated; or the tracking error keeps decreasing in which case a new zooming-in will eventually be triggered.

Combined behavior: Let us now look at the combined behavior of zooming-in and zooming-out phases for the function V and the sets

$$\begin{aligned}
\mathscr{B}_1(\bar{\mu}) &:= \left\{e : |e|\le N\bar{\mu}M\right\}\\
\mathscr{I}_1(\bar{\mu}) &:= \left\{e : e^Te\le N^2\bar{\mu}^2M^2\right\}\\
\mathscr{B}_2(\bar{\mu}) &:= \left\{e : |e|\le N\bar{\mu}R\Delta\right\}\\
\mathscr{I}_2(\bar{\mu}) &= \left\{e : e^Te\le N^2\bar{\mu}^2R^2\Delta^2\right\},
\end{aligned} \tag{39}$$

where $\bar{\mu}$ is taken as the maximum μ_i among all systems i in the network, i.e. $\bar{\mu}=\max_i\mu_i$. Now, provided that the same design parameters M, Δ and R are chosen for all units, including the same initial condition $\mu_i(0)=1$, it is possible to extend the stability argument to the whole Lyapunov function V. In fact, for $t\ge t_0$ (taken as the maximum among all systems), at both zooming-in and zooming-out phases it holds $\dot{V}\le 0\implies V(t)\le V(t_0)$, thus V is upper-bounded by $V(t_0)$ and lower-bounded by 0. Because $\ddot{V}$ is bounded and V is lower bounded by $V(t_0)$, because it holds $\dot{V}\le 0\ \forall t\ge t_0$, we can conclude using the Barbalat's lemma that $\lim_{t\to\infty}\dot{V}(t)=0$.

The following relation from (32) holds:

$$\begin{aligned}
\lim_{t\to\infty}\dot{V}(t) &\le -2\lim_{t\to\infty}\left\|e(t)\right\|\underline{\sigma}(I_N+\mathscr{L})\Big(\left\|e(t)\right\|-\bar{\mu}(t)NR\Delta\Big)\implies\\
0 &\le -2\lim_{t\to\infty}\left\|e(t)\right\|\underline{\sigma}(I_N+\mathscr{L})\Big(\left\|e(t)\right\|-\bar{\mu}(t)NR\Delta\Big).
\end{aligned} \tag{40}$$

The above relation is true when

$$\lim_{t\to\infty}\left\|e(t)\right\|=0\ \text{ or }\ \lim_{t\to\infty}\left\|e(t)\right\|-\bar{\mu}(t)NR\Delta\le 0. \tag{41}$$

The second relation implies that $e\in\mathscr{B}_2(\bar{\mu})$. However when $e\in\mathscr{I}_2(\bar{\mu})$, and because $\mathscr{I}_2(\bar{\mu})\supset\mathscr{B}_2(\bar{\mu})$, $\bar{\mu}$ is decreasing as in (38) because zooming-in occurs, and consequently $e\notin\mathscr{B}_2(\bar{\mu})$. As a consequence $\lim_{t\to\infty}\bar{\mu}(t)=0$ and by (41) we conclude $\lim_{t\to\infty}\left\|e(t)\right\|=0$. □

A state flow diagram of the adaptive hybrid control strategy, with rules for zooming in/out, is shown in Fig. 2.

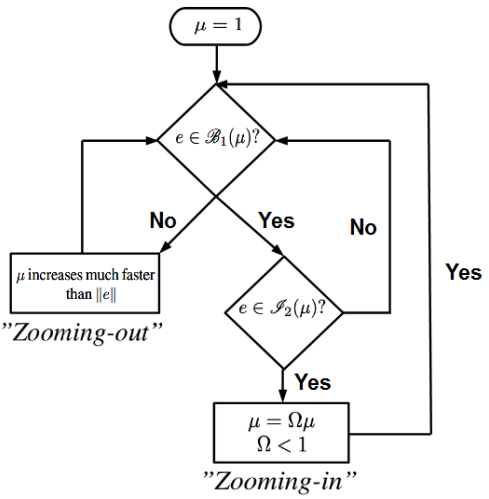

Fig. 2: Error dependent adaptive hybrid control strategy, with rules for zooming in/out.

Some remarks follow.

Remark 7. *The peculiar feature and contribution of the zooming procedure of Theorem 2 is to adopt a Lyapunov function* (19) *that*

allows distributing the quantization strategy throughout the network. In other words, thanks to the diagonal structure of V in (19) *and to the diagonal structure of $\dot{V}$ in* (32) *each system can implement its own zooming strategy only by using measurements from neighbors.*

Remark 8. *Even though the adaptive hybrid synchronization protocol in Theorem 2 is distributed, it requires some global knowledge in order to obtain the parameter R in* (32)*. In particular, some global knowledge of the uncertainty set Θ_i for all units is required in order to obtain $\max_{m_i\in\Theta, i\in\mathcal{V}} \left\| 1+\frac{\tilde{l}_i}{m_i} \right\|$: this global knowledge can be obtained after assuming that all units have the same uncertainty set. In addition, the knowledge of $\overline{\sigma}(I_N+\mathscr{L})$ and of $\underline{\sigma}(I_N+\mathscr{L})$ is required in order to obtain R: it is important to remark that appropriate upper and lower bound for $\overline{\sigma}(I_N+\mathscr{L})$ and for $\underline{\sigma}(I_N+\mathscr{L})$ can be obtained by simply knowing the number of units in the network, or the maximum number of neighbors for each unit. In fact, conservative bounds in this direction can be found in [45–47]. In other words, it is not necessary to know the exact topology of the network in order to estimate $\overline{\sigma}(I_N+\mathscr{L})$ and $\underline{\sigma}(I_N+\mathscr{L})$, and therefore to estimate R.*

Remark 9. *Differently from the non-adaptive zooming procedure [23, 48], where a unique zooming-in occurs, in the adaptive case we might have multiple zooming-in and zooming-out phases. This is because the Lyapunov function* (19) *is quadratic in both the synchronization and the parameter estimation error. Therefore, $\dot{V}\leq 0$ might be due not only to a decreasing synchronization error (eventually leading to zooming-in), but also to decreasing parameter error combined with increasing synchronization error (eventually leading to a new zooming-out). Therefore, convergence of μ may be not monotonic. This is illustrated by the numerical example in the next section.*

Remark 10. *From the dynamics in* (24) *we can see that the quantization of the phase θ_i does not contribute to stability or instability of the adaptive loop: in fact, being the phase always bounded in $[0,2\pi]$, the quantization of θ_i simply acts as a bounded disturbance that can be handled by parameter projection. It is the quantization of $\dot{\theta}_i$ that must be carefully handled in order not to lead to instability. As a matter of fact, if one is interested only in bounded synchronization (in place of asymptotic synchronization), one can have a static quantizer for θ_i and a dynamic quantizer for $\dot{\theta}_i$: using similar steps as in the proof of Theorem 2, one would be able to conclude global uniformly ultimately boundedness of the synchronization error, where the ultimate bound would depend on the precision of the static quantizer for θ_i.*

5 Numerical example

Simulations using the adaptive synchronization protocol of Theorem 1 and the adaptive hybrid synchronization protocol of Theorem 2 are carried out in the following, considering the weighted graph shown in Figure 3. The parameters and initial conditions for each heterogeneous Kuramoto unit (3) are reported in Table 1. Please recall that the unit parameters are unknown to the designer, i.e. the values of Table 1 are used for simulations but not for control design.

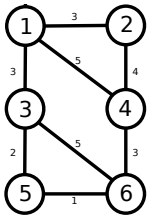

Fig. 3: The Kuramoto undirected weighted graph. The weights k_{ij} are indicated on the links.

Table 1 Parameters and initial conditions for the Kuramoto units.

	m_i	d_i	ω_i	$\theta_i(0)$	$\dot{\theta}_i(0)$
unit #1	1.1	0.1	5	0	0.6
unit #2	1.3	0.15	10	π	0.5
unit #3	1.2	0.2	15	$\pi/2$	0.4
unit #4	1.8	0.21	20	$(5/4)\pi$	0.3
unit #5	1.5	0.25	25	$\pi/4$	0.2
unit #6	1	0.3	30	$(3/2)\pi$	0.1

The reference model is chosen as an integrator with initial condition $x_m(0)=1$ (representing the frequency to be followed). The adaptive gain is taken as $\gamma=1$. The projection bounds are chosen as: $k_i\in[0.05,\ 4]$, $l_i\in[0.8,\ 2]$, $c_i\in[-32,\ -2]$, and $g_{ij}\in[0,\ 6]$. The estimated control gains are initialized as $k_i(0)=0.2$, $l_i(0)=1.5$, $c_i(0)=-10$, $g_{ij}(0)=0$. The parameters for the quantizer are $M=10$ and $\Delta=0.01$: in addition, the parameter R has been calculated as 79.2 (resulting in $\Omega=0.0792$), and the dynamic ranges are initialized as $\mu_i(0)=1$. Clearly, condition (37) is satisfied, therefore Theorem 2 is applicable.

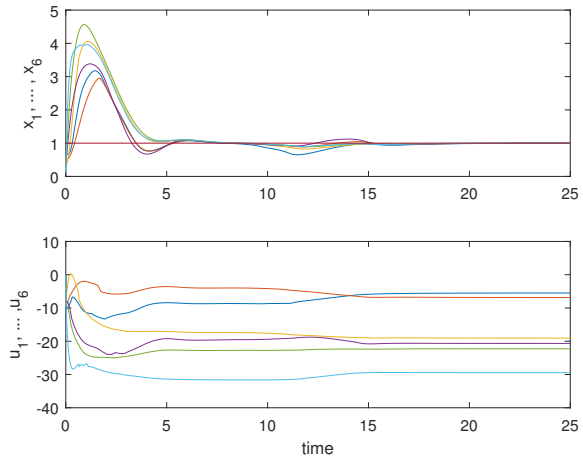

Fig. 4: Adaptive synchronization: synchronization of the frequencies of each unit i to the reference frequency, and control inputs u_i.

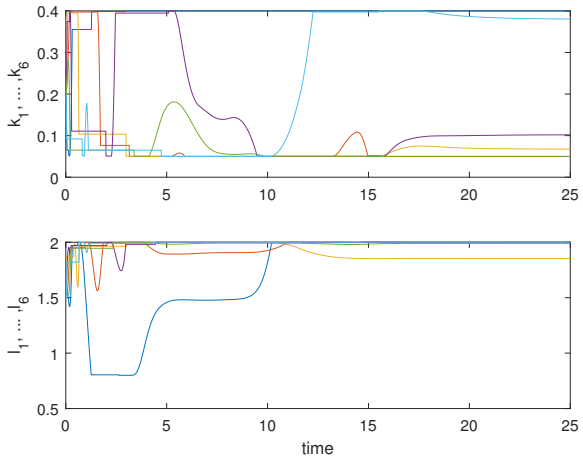

Fig. 5: Adaptive synchronization: adaptive gains k_i and l_i.

The adaptive synchronization resulting from Theorem 1 is shown in Figure 4. Synchronization is achieved and it can be noted that

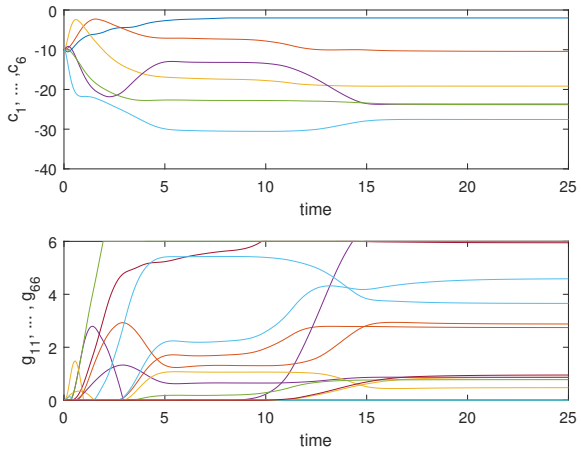

Fig. 6: Adaptive synchronization: adaptive gains c_i and g_{ij}.

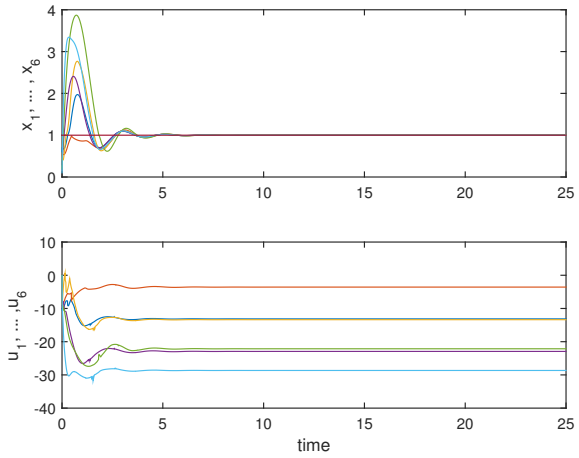

Fig. 7: Adaptive hybrid synchronization: synchronization of the frequencies of each unit i to the reference frequency, and control inputs u_i.

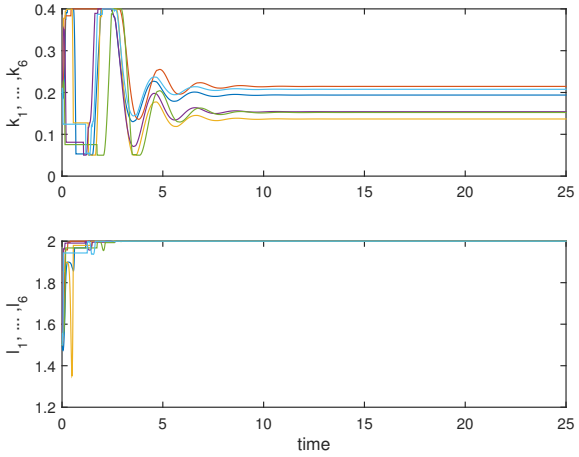

Fig. 8: Adaptive hybrid synchronization: adaptive gains k_i and l_i.

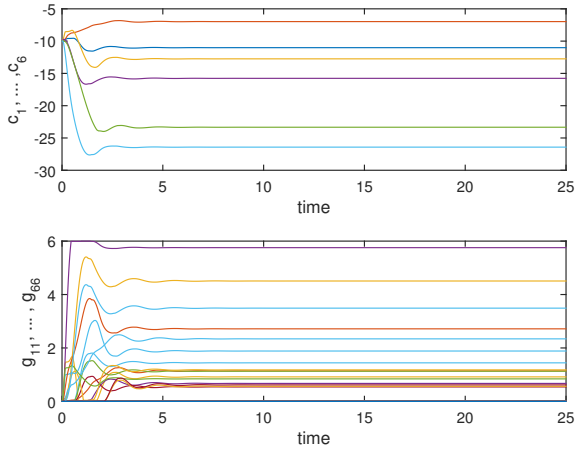

Fig. 9: Adaptive hybrid synchronization: adaptive gains c_i and g_{ij}.

each unit has different control inputs u_i that reach different steady-state values: this is due to heterogeneity, since each unit might need to converge to different steady-state values in order to track the reference frequency. The adaptive gains are reported in Figure 5 and Figure 6, which can be shown to be projected inside their bounds. It can be noted that the weights g_{ij} are not necessarily symmetric $g_{ij} \neq g_{ji}$: this is because, in order to compensate for heterogeneity, the adaptive laws might converge to different values. The adaptive synchronization resulting from Theorem 2 is shown in Figure 7. Synchronization is achieved and, to some extent, convergence is similar to the previous results. The initial transient is slightly different, as it can be noted from the different control inputs u_i. The adaptive gains are reported in Figure 8 and Figure 9. It is important to note that the gains do not necessarily converge to the same values as in the previous simulation: this is a well-know result in adaptive control approaches, since, in the absence of a persistency of excitation condition, convergence of the tracking error to zero might be achieved without the need to converge to the actual parameters (cf. [24–30] and references therein). In other words, adaptive synchronization does not require k_i, l_i, c_i and g_{ij} to converge to k_i^*, l_i^*, c_i^* and g_{ij}^*. Finally, Figure 10 reports how the dynamic range μ_i for each unit evolves with time: after starting from 1, the different μ_i's converge, with different trends, quite fast to small values, which in turn guarantees high quantization precision and asymptotic tracking. Overall, the proposed protocols show the capability to synchronize, in a distributed way, uncertain and heterogeneous units, even in the presence of limited (quantized) information.

By selecting the parameters for the quantizer to be $M = 10$ and $\Delta = 0.1$, we now have $\Omega = 0.792$. This means that the zooming-in is smaller than in the previous case (with $\Delta = 0.01$ we obtained $\Omega = 0.0792$). Figure 11 and Figure 12 show the new synchronization and dynamic range (adaptive gains are not reported for lack of space): it can be seen that asymptotic synchronization is still reached, but the dynamic range takes a bit more time to decrease towards zero. Finally, in order to clarify the benefits of the proposed method, we provide the synchronization with a static quantizer (with no zooming-based strategy). The tracking error can be seen in Figure 13, where it is clear from the zoomed part that the static quantization error will lead to bounded synchronization, in place of asymptotic synchronization.

6 Conclusions

In this work we have studied adaptive synchronization in networks with Kuramoto units whose parameters are unknown and where information is quantized over the communication network. In the presence of both heterogeneous and uncertain dynamics, synchronization has been enabled via appropriate adaptive protocols that counteract the effect of heterogeneity and uncertainty. In particular, to address quantized information, a dynamic quantizer was introduced and embedded into the adaptive mechanism via a zooming-based approach. The resulting protocol ended up being an adaptive hybrid control strategy, for which synchronization to a

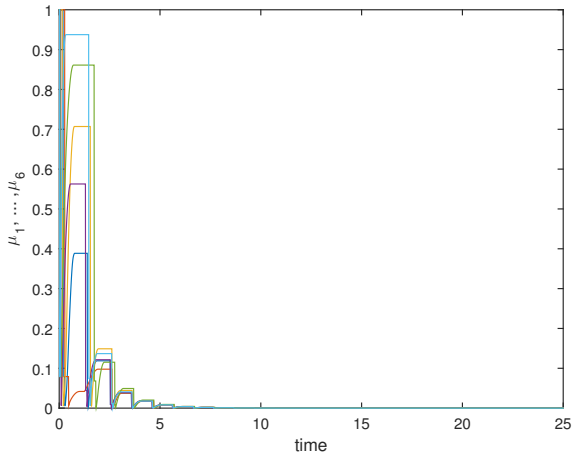

Fig. 10: Adaptive hybrid synchronization: dynamic range μ_i for each unit i.

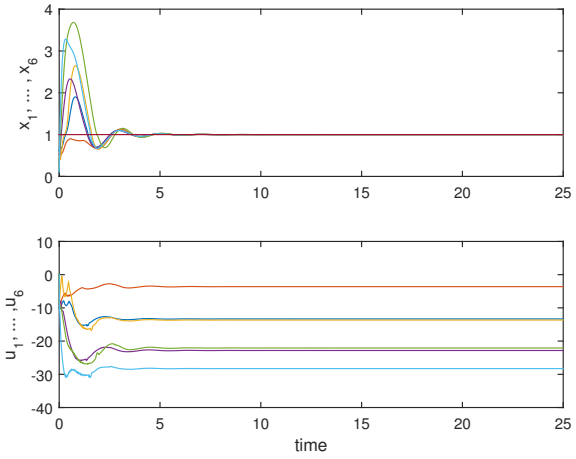

Fig. 11: Adaptive hybrid synchronization with $\Delta = 0.1$: synchronization of the frequencies of each unit i to the reference frequency, and control inputs u_i.

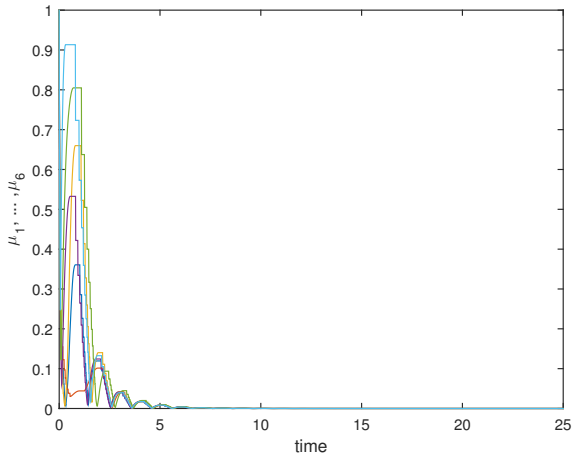

Fig. 12: Adaptive hybrid synchronization with $\Delta = 0.1$: dynamic range μ_i for each unit i.

desired frequency was shown via Lyapunov analysis. Finally, numerical examples have demonstrated the effectiveness of the proposed protocol.

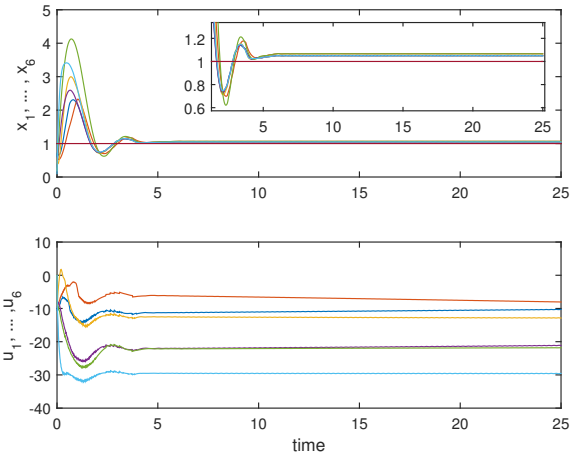

Fig. 13: Static quantizer synchronization: synchronization of the frequencies of each unit i to the reference frequency, and control inputs u_i.

Future work might include the following aspects: in smart grids, which are a typical application field of Kuramoto networks, it is often of practical interest to optimize the power flow: this implies satisfying some constraints on the phase differences between unit [49, 50]. This aspect has not been addressed in this work and would be of interest for future work. Also, some practical input constraints like input saturation or discrete inputs are of interest in view of: the limits of generation or load shedding, or some possibly discrete generation or load shedding actions [51]. An adaptive approach in this direction has been recently investigated in [52], even though the extension to network systems is open. Other networked-induced constraints like sampled information have been studied in [53], although adaptivity to parametric uncertainty has not been covered. All these aspects are of extreme interest for future work.

Acknowledgments

Mr. Ilario Azzollini and Dr. Shuai Yuan are gratefully acknowledged for useful discussions on the topics of this work. The research leading to these results has been partially funded by the European Commission H2020-SEC-2016-2017-1, Border Security: autonomous systems and control systems, under contract #740593 (ROBORDER) and H2020-ICT-2014-1, FIRE+ (Future Internet Research & Experimentation), under contract #645220 (RAWFIE).

7 References

1 A. Jadbabaie, J. Lin, and A. S. Morse, "Coordination of groups of mobile autonomous agents using nearest neighbor rules," *IEEE Transactions on Automatic Control*, vol. 48, no. 6, pp. 988–1001, 2003.

2 R. Olfati-Saber, J. A. Fax, and R. M. Murray, "Consensus and cooperation in networked multi-agent systems," *Proceedings of the IEEE*, vol. 95, no. 1, pp. 215–233, 2007.

3 Y. A. Harfouch, S. Yuan, and S. Baldi, "An adaptive switched control approach to heterogeneous platooning with inter-vehicle communication losses," *IEEE Transactions on Control of Network Systems*, vol. PP, no. 99, pp. 1–1, 2017.

4 X. F. Wang and G. Chen, "Synchronization in scale-free dynamical networks: robustness and fragility," *IEEE Transactions on Circuits and Systems I: Fundamental Theory and Applications*, vol. 49, no. 1, pp. 54–62, 2002.

5 P. Wieland, R. Sepulchre, and F. Allgower, "An internal model principle is necessary and sufficient for linear output synchronization," *Automatica*, vol. 47, no. 5, pp. 1068 – 1074, 2011.

6 P. Lu, W. Yu, and F. Zhang, "Leader-follower formation control with mismatched compasses," in *2017 36th Chinese Control Conference (CCC)*, 2017, pp. 8821–8826.

7 F. Sorrentino, M. di Bernardo, F. Garofalo, and G. Chen, "Controllability of complex networks via pinning," *Physical Review E*, vol. 75, pp. 1–6, 2007.

8 Y. Kuramoto, *Chemical Oscillations, Waves, and Turbulence*. Springer, 1984.

9 I. D. Couzin, J. Krause, N. R. Franks, and S. A. Levin, "Effective leadership and decision-making in animal groups on the move," *Nature*, vol. 433, pp. 513 – 516, 2005.

10 F. Dorfler and F. Bullo, "Synchronization in complex networks of phase oscillators: A survey," *Automatica*, vol. 50, no. 6, pp. 1539 – 1564, 2014.
11 A. R. Bergen and D. J. Hill, "A structure preserving model for power system stability analysis," *IEEE transactions on power apparatus and systems*, vol. 100, pp. 25–35, 1981.
12 M. Okaniwa and H. Ishii, "An averaging method for synchronization in Kuramoto models," *3rd IFAC Workshop on Distributed Estimation and Control in Networked Systems*, vol. 45, no. 26, pp. 282 – 287, 2012.
13 F. Dorfler, M. Chertkov, and F. Bullo, "Synchronization in complex oscillator networks and smart grids," *Proceedings of the National Academy of Sciences*, vol. 110, no. 6, pp. 2005–2010, 2013.
14 T. Gross and B. Blasius, "Adaptive coevolutionary networks: a review," *Journal of The Royal Society Interface*, vol. 5, no. 20, pp. 259–271, 2008.
15 S. Baldi, "Cooperative output regulation of heterogeneous unknown systems via passification-based adaptation," *IEEE Control Systems Letters*, vol. 2, no. 1, pp. 151–156, 2018.
16 I. A. Azzollini, S. Baldi, and E. B. Kosmatopoulos, "Adaptive synchronization in networks with heterogeneous uncertain kuramoto-like units," in *2018 European Control Conference, June 12th-15th, Limassol, Cyprus*, 2018.
17 S. Assenza, R. Gutierrez, J. Gomez-Gardenes, V. Latora, and S. Boccaletti, "Emergence of structural patterns out of synchronization in networks with competitive interactions," *Scientific Reports*, vol. 1, no. 99, pp. 1 – 8, 2011.
18 P. D. Lellis, M. D. Bernardo, F. Sorrentino, and A. Tierno, "Adaptive synchronization of complex networks," *International Journal of Computer Mathematics*, vol. 85, no. 8, pp. 1189–1218, 2008.
19 Q. Ren, M. He, X. Yu, Q. Long, and J. Zhao, "The adaptive coupling scheme and the heterogeneity in intrinsic frequency and degree distributions of the complex networks," *Physics Letters A*, vol. 378, no. 3, pp. 139 – 146, 2014.
20 S.-Y. Ha, S. E. Noh, and J. Park, "Synchronization of Kuramoto oscillators with adaptive couplings," *SIAM Journal on Applied Dynamical Systems*, vol. 15, no. 1, pp. 162–194, 2016.
21 L. Papadopoulos, J. Z. Kim, J. Kurths, and D. S. Bassett, "Development of structural correlations and synchronization from adaptive rewiring in networks of Kuramoto oscillators," *Chaos*, vol. 27, no. 7, p. 073115, 2017.
22 H. Ishii and B. A. Francis, "Quadratic stabilization of sampled-data systems with quantization," *Automatica*, vol. 39, no. 10, pp. 1793–1800, 2003.
23 D. Liberzon, "Hybrid feedback stabilization of systems with quantized signals," *Automatica*, vol. 39, no. 9, pp. 1543–1554, 2003.
24 A. Selivanov, A. Fradkov, and D. Liberzon, "Adaptive control of passifiable linear systems with quantized measurements and bounded disturbances," *Systems & Control Letters*, vol. 88, pp. 62–67, 2016.
25 T. Hayakawa, H. Ishii, and K. Tsumura, "Adaptive quantized control for nonlinear uncertain systems," *Systems & Control Letters*, vol. 58, no. 9, pp. 625–632, 2009.
26 N. Moustakis, S. Yuan, and S. Baldi, "An adaptive approach to zooming-based control for uncertain systems with input quantization," in *2018 European Control Conference, June 12th-15th, Limassol, Cyprus*, 2018.
27 T. Hayakawa, H. Ishii, and K. Tsumura, "Adaptive quantized control for linear uncertain discrete-time systems," *Automatica*, vol. 45, no. 3, pp. 692 – 700, 2009.
28 N. Moustakis, S. Yuan, and S. Baldi, "An adaptive design for quantized feedback control of uncertain switched linear systems," *International Journal of Adaptive Control and Signal Processing*, 2018.
29 X. Yu and Y. Lin, "Adaptive backstepping quantized control for a class of nonlinear systems," *IEEE Transactions on Automatic Control*, vol. 62, no. 2, pp. 981–985, 2017.
30 L. Huang, Y. Li, and S. Tong, "Command filter-based adaptive fuzzy backstepping control for a class of switched non-linear systems with input quantisation," *IET Control Theory Applications*, vol. 11, no. 12, pp. 1948–1958, 2017.
31 G. Lai, Z. Liu, C. L. P. Chen, and Y. Zhang, "Adaptive asymptotic tracking control of uncertain nonlinear system with input quantization," *Systems & Control Letters*, vol. 96, pp. 23–29, 2016.
32 R. Carli, F. Fagnani, P. Frasca, and S. Zampieri, "Gossip consensus algorithms via quantized communication," *Automatica*, vol. 46, no. 1, pp. 70 – 80, 2010.
33 P. Frasca, R. Carli, F. Fagnani, and S. Zampieri, "Average consensus on networks with quantized communication," *International Journal of Robust and Nonlinear Control*, vol. 19, no. 16, pp. 1787–1816, 2009.
34 P. Frasca, "Continuous-time quantized consensus: Convergence of krasovskii solutions," *Systems & Control Letters*, vol. 61, no. 2, pp. 273 – 278, 2012.
35 Z. Li, Z. Duan, G. Chen, and L. Huang, "Consensus of multiagent systems and synchronization of complex networks: A unified viewpoint," *IEEE Transactions on Circuits and Systems I: Regular Papers*, vol. 57, no. 1, pp. 213–224, 2010.
36 A. Abdessameud, A. Tayebi, and I. G. Polushin, "Attitude synchronization of multiple rigid bodies with communication delays," *IEEE Transactions on Automatic Control*, vol. 57, no. 9, pp. 2405–2411, 2012.
37 Q. Song, F. Liu, J. Cao, and W. Yu, "*m*-matrix strategies for pinning-controlled leader-following consensus in multiagent systems with nonlinear dynamics," *IEEE Transactions on Cybernetics*, vol. 43, no. 6, pp. 1688–1697, 2013.
38 Y. Wang and F. J. Doyle, "Exponential synchronization rate of kuramoto oscillators in the presence of a pacemaker," *IEEE Transactions on Automatic Control*, vol. 58, no. 4, pp. 989–994, 2013.
39 X. Li and P. Rao, "Synchronizing a weighted and weakly-connected kuramoto-oscillator digraph with a pacemaker," *IEEE Transactions on Circuits and Systems I: Regular Papers*, vol. 62, no. 3, pp. 899–905, 2015.
40 G. Filatrella, A. H. Nielsen, and N. F. Pedersen, "Analysis of a power grid using a Kuramoto-like model," *The European Physical Journal B*, vol. 61, no. 4, pp. 485–491, 2008.
41 J. Giraldo, E. Mojica-Nava, and N. Quijano, "Synchronization of dynamical networks with a communication infrastructure: A smart grid application," in *52nd IEEE Conference on Decision and Control*, 2013, pp. 4638–4643.
42 M. Lu and L. Liu, "Distributed feedforward approach to cooperative output regulation subject to communication delays and switching networks," *IEEE Transactions on Automatic Control*, vol. 62, no. 4, pp. 1999–2005, 2017.
43 H. Cai, F. L. Lewis, G. Hu, and J. Huang, "The adaptive distributed observer approach to the cooperative output regulation of linear multi-agent systems," *Automatica*, vol. 75, pp. 299 – 305, 2017.
44 Z. Feng, G. Hu, W. Ren, W. E. Dixon, and J. Mei, "Distributed coordination of multiple unknown euler-lagrange systems," *IEEE Transactions on Control of Network Systems*, vol. PP, no. 99, pp. 1–1, 2016.
45 Y. Hong and C.-T. Pan, "A lower bound for the smallest singular value," *Linear Algebra and its Applications*, vol. 172, pp. 27 – 32, 1992.
46 M. Franceschelli, A. Gasparri, A. Giua, and C. Seatzu, "Decentralized estimation of laplacian eigenvalues in multi-agent systems," *Automatica*, vol. 49, no. 4, pp. 1031 – 1036, 2013.
47 C. P. Bechlioulis and G. A. Rovithakis, "Decentralized robust synchronization of unknown high order nonlinear multi-agent systems with prescribed transient and steady state performance," *IEEE Transactions on Automatic Control*, vol. 62, no. 1, pp. 123–134, 2017.
48 S. Yuan and S. Baldi, "Stabilization of switched linear systems using quantized output feedback via dwell-time switching," in *2017 13th IEEE International Conference on Control Automation (ICCA)*, 2017, pp. 236–241.
49 S. Jafarpour and F. Bullo, "Synchronization of Kuramoto Oscillators via Cutset Projections," *ArXiv e-prints*, 2017.
50 P. Rao, X. Li, and M. J. Ogorzalek, "Stability of synchronous solutions in a directed kuramoto-oscillator network with a pacemaker," *IEEE Transactions on Circuits and Systems II: Express Briefs*, vol. 64, no. 10, pp. 1222–1226, 2017.
51 J. Giraldo, E. Mojica-Nava, and N. Quijano, "Tracking of kuramoto oscillators with input saturation and applications in smart grids," in *2014 American Control Conference*, 2014, pp. 2656–2661.
52 S. Yuan, L. Zhang, O. Holub, and S. Baldi, "Switched adaptive control of air handling units with discrete and saturated actuators," *IEEE Control Systems Letters*, vol. 2, no. 3, 2018.
53 J. Giraldo, E. Mojica-Nava, and N. Quijano, "Synchronisation of heterogeneous kuramoto oscillators with sampled information and a constant leader," *International Journal of Control*, pp. 1–17, 2018.